Hybrid PET/MRI in Staging Endometrial Cancer: Diagnostic and Predictive Value in a Prospective Cohort

Gabriele Ironi
Department of Radiology, IRCCS San Raffaele Scientific Institute, Milan, Italy
Paola Mapelli
Vita-Salute San Raffaele University, Milan, Italy; Nuclear Medicine Department, IRCCS San Raffaele Scientific Institute, Milan, Italy
Alice Bergamini
Vita-Salute San Raffaele University, Milan, Italy; Obstetrics and Gynecology Unit, IRCCS San Raffaele Scientific Institute, Milan, Italy
Federico Fallanca
Nuclear Medicine Department, IRCCS San Raffaele Scientific Institute, Milan, Italy
Giorgio Candotti
Vita-Salute San Raffaele University, Milan, Italy; Obstetrics and Gynecology Unit, IRCCS San Raffaele Scientific Institute, Milan, Italy
Chiara Gnasso
Department of Radiology, IRCCS San Raffaele Scientific Institute, Milan, Italy; Vita-Salute San Raffaele University, Milan, Italy
Gianluca Taccagni
Pathology Unit, IRCCS San Raffaele Scientific Institute, Milan, Italy
Miriam Sant'Angelo
Pathology Unit, IRCCS San Raffaele Scientific Institute, Milan, Italy
Paola Scifo
Nuclear Medicine Department, IRCCS San Raffaele Scientific Institute, Milan, Italy
Carolina Bezzi
Vita-Salute San Raffaele University, Milan Italy; Nuclear Medicine Department, IRCCS San Raffaele Scientific Institute, Milan, Italy
Paola Maria Vittoria Rancoita
University Centre of Statistics in the Biomedical Sciences, Vita-Salute San Raffaele University, Milan, Italy
Giorgia Mangili
Obstetrics and Gynecology Unit, IRCCS San Raffaele Scientific Institute, Milan, Italy
Luca Bocciolone

Obstetrics and Gynecology Unit, IRCCS San Raffaele Scientific Institute, Milan, Italy

Massimo Candiani

Obstetrics and Gynecology Unit, IRCCS San Raffaele Scientific Institute, Milan, Italy

Luigi Gianolli

Nuclear Medicine Department, IRCCS San Raffaele Scientific Institute, Milan, Italy

Francesco De Cobelli

Department of Radiology, IRCCS San Raffaele Scientific Institute, Milan, Italy; Vita-Salute San Raffaele University, Milan, Italy

Maria Picchio (picchio.maria@hsr.it)

Vita-Salute San Raffaele University https://orcid.org/0000-0002-7532-6211

Research Article

Keywords: 18F-FDG PET/MRI, Endometrial cancer, Preoperative staging, Pelvic malignancies, Predictive value

Posted Date: June 22nd, 2021

DOI: https://doi.org/10.21203/rs.3.rs-630871/v1

Version of Record: A version of this preprint was published at Clinical Nuclear Medicine on January 21st, 2022. See the published version at https://doi.org/10.1097/RLU.0000000000004064.

Abstract

Purpose. Assessment of deep myometrial invasion (MI) and lymphovascular space invasion (LVSI) is of utmost importance in preoperative staging of endometrial cancer (EC). Imaging parameters derived respectively from MRI and PET have shown good predictive value. Aim of the present study is to assess the diagnostic performance of hybrid 18F-FDG PET/MRI in EC staging, with particular focus on MI and LVSI detection.

Methods. Prospective monocentric study including 35 patients with biopsy-proven EC undergoing preoperative 18F-FDG PET/MRI for staging purpose. Histological examination was the reference standard. PET (SUVmax, SUVmean40, MTV40, TLG40) and MRI (volume index-VI, total tumor volume-TTV, tumor volume ratio-TVR, ADCmean, ADCmin) parameters were calculated on the primary tumor, and their role in predicting histological findings (grade, high- vs. low-risk groups, LVSI, MI, p53 hyper-expression) was assessed through a ROC analysis.

Results. 18F-FDG-PET/MRI identified the primary tumor in all patients. In the LVSI detection, PET/MRI demonstrated high accuracy, specificity and negative predictive value (sensitivity=0.8571, specificity=0.9286, accuracy=0.9143, NPV=0.9630, PPV=0.7500). Assessment of MI using PET/MRI correctly staged 27 patients, showing a good positive predictive value (77.1%; sensitivity= 0.7273, specificity=0.8462, accuracy=0.7714, PPV=0.8889, NPV=0.647). VI, TTV, and TVR significantly predicted risk groups (p=0.0059, 0.0235, 0.0181, respectively). VI, TTV, TVR, MTV40 and TLG40 significantly predicted LVSI (p=0.0023, 0.0068, 0.0068, 0.0027, 0.0139, respectively). Imaging was not able to predict grading, MI nor p53 hyper-expression.

Conclusion. 18F-FDG-PET/MRI has good accuracy in preoperative staging of EC; PET and MRI parameters have synergic role in preoperatively predicting LVSI, with MRI parameters being also predictive for EC risk groups.

Introduction

Endometrial cancer is one of the most frequent cancers worldwide [1–6]. Although most endometrial tumors are diagnosed at an early stage, the 5-year overall survival (OS) remains highly variable, 85–90% for stage I, 75–85% for stage II, 50–56% for stage III and 20–25% for stage IV, regardless of tumor type [7]. Prognosis and therapeutic strategy are currently defined by histomorphology classification into type I (80–90% of cases), which includes endometrial adenocarcinoma, and type II (10–20% of cases) including non-endometrioid subtypes, such as serous, clear-cell and undifferentiated carcinomas [2, 4, 6, 7].

Specific intrinsic disease characteristics also influence outcome. In stage I patients, elevated myometrial invasion (> 50%) and tumor grade (III) play a further discriminating factor on prognosis and increases the risk of pelvic and distant recurrence with a significant difference in 5-year survival which is reduced to

58% [8–10]. The 5-year OS of patients with non-endometrioid serous tumors (20–25%), usually diagnosed at later stages in which extrauterine disease is present in 60–70% of cases, is poor [7, 11–13].

Surgical intervention is commonly planned based on information provided by preoperative biopsy (histotype, tumor grade) and morphological imaging derived data (such as myometrial invasion and lymph node involvement). However, basal histotype may be elusive due to intrinsic tumor heterogeneity which may not be represented in the biopsy sampled tissue[14, 15]. Current guidelines also indicate the best adjuvant therapies based on precisely defined risk groups which derive from histopathology [6, 7].

Magnetic resonance imaging (MRI) provides high soft tissue contrast and is particularly useful in local staging of the disease. MRI can accurately assess the depth of myometrial invasion which can impact on patient management and aid in stratifying patients into low versus intermediate risk groups before surgery [6, 16–18].

18F-fluorodeoxyglucose (18F-FDG) positron emission tomography/computed tomography (PET/CT) has been shown to well correlate with endometrial cancer aggressiveness, including assessment of lymph node involvement; however, this functional modality presents limitations in detecting microscopic metastases [18–20].

Evaluation of deep myometrial invasion and lymph node involvement derived respectively from MRI and PET studies in patients with endometrial cancer has shown to have good predictive value [21, 22].

In such a complex scenario, the use of a fully integrated PET/MRI scanners, which combines high contrast resolution of soft tissue from MRI with metabolic information deriving from the PET component, is an undoubtfully advantageous providing an accurate local staging and whole-body staging of the disease.

The aim of the present study is to evaluate the performance of hybrid 18F-FDG PET/MRI in staging endometrial cancer patients. In particular, the diagnostic accuracy of this modality in detecting the depth of myometrial invasion and the presence of lymph node metastases in patients with endometrial cancer candidate to surgery will be investigated. In addition, the prognostic value of specific PET and MRI derived parameters in detecting the risk of disease recurrence and disease aggressiveness will also be assessed.

Materials And Methods

Patients

This is a single center prospective cohort study carried out at San Raffaele Scientific Institute.

All consecutive female patients presenting to the Hospital’s Department of Obstetrics and Gynecology with histopathological confirmation of primary endometrial cancer, scheduled to 18F-FDG PET/MRI and candidate to surgical intervention have been enrolled in the study between December 2018 and January

2021. Data was right censored on March 31st, 2021. Informed consent was obtained from all participants prior to inclusion. Clinical history, demographic data and histology were collected. Follow-up data collected until March 2021 included imaging, clinical and laboratory data, need of adjuvant therapy (chemotherapy and/or external beam radiation therapy).

A dichotomous classification of risk was used to define low- and high-risk groups according to the ESMO-ESGO-ESTRO consensus conference[6]: patients with type 1, stage 1 and grade 1–2 and negative for LVSI were regarded as low-risk; the remaining patients were included in the high-risk group. Deep myometrial invasion was defined as myometrial invasion > 50%.

The study was approved by the Institution's Ethics Committee (protocol number 85/INT/2019). All procedures were carried out in accordance with the Declaration of Helsinki (1964) and its later amendments; informed consent was collected from all patients according to EC guidelines.

PET/MR Imaging acquisition

All scans were performed using a fully hybrid 3T PET/MRI system (SIGNA PET, General Electric Medical Systems, Wakesha, Wisconsin, USA).

A simultaneous PET/MRI Whole Body (WB) scan was acquired approximately 60 minutes (range 60–90) after i.v. administration of 18F labelled deoxy-glucose (18F-FDG).The dose injected was calculated following the EANM procedure guidelines for tumor imaging[23]. The acquisition protocol started with MR localizers, in order to define the number of table positions (PET-FOV) needed to cover the spatial range for the WB study. PET acquisition was performed in the 3D list mode (4min/PET-FOV) to ensure extensive data handling during image reconstruction. Simultaneously, a two-Point Dixon MR sequence was acquired (for each PET-FOV) for the attenuation correction of the corresponding PET data. LAVA-Flex (LAVA: liver acquisition with volume acceleration) sequences were also acquired over the WB scan range and used for anatomical localization of the PET signal.

At the end of the WB scan and after a brief break, a dedicated single PET-FOV centered on the pelvic region was acquired. Prior to acquisition, patients were administered 40 mg of hyoscine butyl bromide (Buscopan; Boehringer, Ingelheim, Germany) intramuscularly to reduce artifacts related to bowel motion. The pelvic MRI study included a full set of diagnostic MRI sequences. First, a large FOV axial T2-w imaging of the pelvis (repetition time msec/echo time msec, 8844/150; matrix, 512; number of signals acquired, 2; FOV, 38; section thickness, 5 mm) was acquired. High-resolution small FOV T2-weighted FSE (fast spin echo) PROPELLER (Periodically Rotated Overlapping ParallEL Lines with Enhanced Reconstruction) sequences followed and were acquired in the 3 planes with respect to main axis of the uterus: sagittal (repetition time msec/echo time msec, 8637/140; matrix, 512; number of signals acquired, 3; FOV, 20; section thickness, 3 mm), axial oblique (repetition time msec/echo time msec, 8200/140; matrix, 512; number of signals acquired, 3.5; FOV, 18; section thickness, 3 mm) and coronal oblique (repetition time msec/echo time msec, 8929/140; matrix, 512; number of signals acquired, 3; FOV, 14.1; section thickness, 3 mm). Lastly, a small FOV axial-oblique diffusion-weighted acquisition (DWI-FOCUS)

covering the primary tumor was performed with the following parameters: repetition time msec/echo time msec, 2099/72.8; matrix, 100x50; FOV, 26; section thickness, 3mm; b values, 0–200 – 600–1000 sec/mm^2).

A dynamic contrast enhanced (DCE)-MRI study of the primary tumor was performed after administration of 0.1 mmol/kg of body weight of gadolinium chelate (Gadovist; Bayer, Canada) by using a T1w Spoiled Gradient Recolled Echo (SPGR) DIfferential Sub-sampling with Cartesian Ordering (DISCO) sequence (repetition time msec/echo time msec, 5.167/1.674; matrix, 148x132; number of signals acquired, 1.42; FOV, 29x29; section thickness, 3 mm) with a temporal resolution of 4 sec. Sequential images were obtained before administration of contrast medium to 5 minutes after. Finally, a small FOV high-resolution 3D fat-saturated T1-weighted sequence of the uterus (repetition time msec/echo time msec, 9/1.3; matrix, 268x268; number of signals acquired, 1; FOV, 28; section thickness, 1 mm) was acquired: this data set was subsequently reconstructed with respect to the 3 planes of the uterus in order to obtain accurate delineation of tumor boundaries.

The total acquisition time per patient was approximately 1 hour.

Image Processing and Reconstruction

From the two-Point Dixon MR sequence the resulting images (in-phase, opposed-phase, water-weighted and fat-weighted) were processed for attenuation correction (AC) to generate a four-class segmented map of attenuation coefficients (air, lung, water, fat) used for AC of the corresponding PET data.

PET image reconstruction was performed using a Bayesian penalized likelihood algorithm (Q.Clear-GE) which allows effective convergence of image accuracy while suppressing noise, using a penalty function. The algorithm includes Point Spread Function and Time of Flight models. Twenty-eight subsets and twenty-five iterations were performed to reach signal convergence. The beta parameter, which characterizes the weight of the penalization terms, was independently optimized for Whole Body and high statistics (single FOV) PET scan.

Image analysis

PET images were analyzed by an experienced nuclear medicine physician (F.F. 20 years' experience) and MRI images by an experienced radiologist (G.I. 7 years' experience), both blinded to clinical and instrumental data. A consensus was reached at the end of the evaluations for the production of a combined PET/MRI evaluation and report. Qualitative and quantitative analysis was performed with the Advantage Workstation (ADW Dexus Version 4.7) of both PET and MRI derived data.

Regarding PET image analysis, the presence of pathological 18F-FDG uptake was defined as an increased tracer uptake compared to the tracer distribution in the surrounding tissues and structures, with the exception of areas of physiologically increased uptake. Exact anatomic location of abnormal uptake in the uterus and lymph nodes was identified on the basis of integrated MRI images; lymphnodes were considered positive if 18F-FDG uptake was evident, regardless of their diameter on MR images.

Quantitative analysis of the primary tumor on trans-axial PET images included 3-dimensional volumetric measurements of: maximum standardized uptake value (SUVmax), mean standardized uptake value (SUVmean), Metabolic Tumor Volume (MTV) and Total Lesion Glycolysis (TLG). SUVmax was defined as the maximum activity concentration in the tumor/(injected dose/body weight), MTV as the FDG-avid tumor volume, and TLG as MTV × SUVmean, where SUVmean was defined as the mean concentration of FDG in the tumor/(injected dose/body weight). MTV was obtained as the sum in cubic centimetres of the tumor volume on the FDG PET scan. For SUVmean, MTV and TLG the threshold was set at 40%.

MRI interpretation followed classification of the primary lesion (multiparametric approach combining T2-weighted images, DWI and T1-weighted post-contrast images) according to current guidelines[17, 24]. Pelvic lymph nodes with a short axis diameter greater than 8 mm were classified as malignant[6]. In addition, descriptive morphological criteria (round shape, speculated margins, heterogeneous signal intensity or the presence of internal necrosis) were used to describe other node involvement.

The evaluated quantitative MRI parameters were: volume index (defined as products of maximum anterior-posterior, transverse and cranial-caudal tumor diameters), total tumor volume (TTV), tumor volume ratio (TVR), ADC (apparent diffusion coefficient) -mean and -min. TVR is defined as (TTV/TUV) x 100; TTV is the total tumor volume measured on fat-saturated T1-w post-contrast images (better delineation of lesion boundaries); TUV is total uterine volume measured on high-resolution T2w sagittal images (excluding the cervix and fibroids deforming the outer edge of the uterus). For apparent diffusion coefficient (ADC) calculation, ROIs (regions of interest) were drawn around the tumor on each section on the high b-values images and then these ROIs were copied on the ADC map. Perfusion evaluation and analysis is not described in the present study.

Surgery and histopathological analysis

All patients underwent surgical intervention within 1 month from the 18F-FDG PET/MRI scan. Surgery consisted in total open or laparoscopic hysterectomy, bilateral salpingo-oophorectomy and peritoneal washing. A pathologist specialized in gynecologic oncology (G.T. with more than 30 years of experience), blinded to PET/MRI findings, performed histopathologic examination of all cases with multiple sections for each case. For each case, histotype, grading, level and type of myometrial infiltration pattern, lympho-vascular space invasion (LVSI) were evaluated. In addition, a panel of Immuno-histochemical parameters were also considered: estrogen receptor (ER), progesterone receptor (PGR), p16, p53, Beta-catenin and Micro-Satellite Instability (M.S.I). Positivity for p53 was correlated to wild type or mutational type expression (hyper-expressed or null).

For nodal staging, histopathological findings after pelvic/paraortic lymphadenectomy or sentinel lymph node dissection (SLND) as well as imaging follow-up were used as a reference standard.

Staging was assessed according to the FIGO classification of endometrial tumors.

Statistical analysis

In order to investigate the prognostic role of the fully integrated PET/MRI exam, several parameters extrapolated from the PET and MR images were evaluated with respect to their ability in predicting histological findings after surgery (risk group, deep myometrial invasion, grade, LVSI, p53 hyper-expression) through a Receiver Operating Characteristics (ROC) curve analysis. For each PET/MRI parameter, the optimal cut-off was derived using the standard method, consisting in choosing that value corresponding to the point on the ROC curve nearest to the upper left corner of the ROC graph. For each histological variable, adjustment for multiple comparisons was performed using Bonferroni's correction.

Overall, PET/MRI ability (as a qualitative variable) to detect lymph node involvement and deep myometrial invasion was evaluated with the following indices: sensitivity, specificity, accuracy, positive (PPV) and negative (NPV) predictive value.

P-values less than 0.05 were considered significant. All statistical analyses were performed using R 3.5.0 (http://www.R-project.org/).

Results

Patients' characteristics

A total of 36 women were enrolled in the study, yet only thirty-five women were included in the final analysis as one patient did not follow-through with planned surgery (extensive metastatic disease). Criteria for selection are depicted in Fig.1. Mean age was 66.57 years (SD: 10.21). No adverse events were recorded during the acquisition of the PET/MRI scan and none were reported until end of data collection.

Tumor characteristics defined by histopathological data showed that myometrial invasion greater than 50% was present in 22 patients (62.9%); 13 (37.1%) patients had p53 hyper-expression; 13 (37.1%) had LVSI.

Six patients did not undergo SNL biopsy, sample or lymphadenectomy and were evaluated at defined imaging and clinical time-points (minimum follow-up of these patients 1-year post-surgery). Of these, only one presented lymph node metastasis at 9 months post-surgery imaging. The remaining patients underwent pelvic systematic lymphadenectomy (6), SLND (13) or biopsy sampling (10): in 6 patients' nodal involvement was positive. Therefore, a total of 7 women (20%) had lymph node metastases.

Complete patients' demographics and tumor characteristics based on histopathological data (including Grade and Figo score) are presented in Table 1.

18F-FDG PET/MR image findings

Focal pathological 18F-FDG uptake was detected in correspondence to the primary tumor in all patients (100%). In 8 patients (28%), increased focal uptake was also detected in correspondence of pathological lymph nodes (patient-based).

Median SUVmax, SUVmean40, MTV40 and TLG were respectively 21.51 (IQR 17.2-23.945), 13.31 (IQR 11.03-14.7), 9.39 (IQR 4.505-30.595) and 139.913 (IQR 38.959-434.851).

MRI detected the primary tumor in all patients (100%) and pelvic lymph node involvement was found in 8 patients (patient based; 28%). Primary tumor median TTV, volume index and TVR were 9.47 cc (IQR 3.5 – 42.65), 23.92 cc (IQR 7.66-98.48) and 19.46 cc (IQR 7.23 - 33), respectively; ADCmean and ADCmin values were 0.96 (IQR 0.85 – 1.03) and 0.63 (IQR 0.51 – 0.74), respectively (Fig.2 and Fig.3). Complete imaging-based parameters are reported in Table 2.

18F-FDG PET/MRI performance and predictive value

PET/MRI was able to detect lymphnodal involvement with high accuracy and high specificity (sensitivity=0.8571, specificity=0.9286, accuracy=0.9143). Hybrid imaging also had a high negative predictive value for lymphnodal involvement (NPV=0.9630; PPV=0.7500).

The assessment of deep myometrial invasion using PET/MRI correctly staged 27 patients (77.1%; sensitivity= 0.7273, specificity=0.8462, accuracy=0.7714), with also a good positive predictive value (PPV=0.8889, NPV=0.647).

ROC curve analysis used to investigate the performance of selected PET and MRI quantitative parameters in predicting tumor status or characteristic (derived from histology) well described the prognostic role of PET/MRI. MRI derived volume index, TTV, and TVR were significant in predicting endometrial cancer groups (high risk vs. low-risk patients) (p= 0.0059, 0.0235, 0.0181, respectively; Table 3a). MRI derived volume index, TTV, TVR and PET derived MTV40 and TLG40 were able to predict LVSI (p=0.0023, 0.0068, 0.0068, 0.0027, 0,01394, respectively; Table 3b). Imaging was not able to predict grading, presence of deep myometrial invasion, hyper-expression of p53 (Table 3c-e). ROC curve analysis for positive lymph nodes prediction was not performed due to the small number of events.

Discussion

Imaging has a central and undisputed role in the preoperative evaluation of patients with endometrial cancer [25–27] and the ESMO-ESGO-ESTRO consensus conference highlighted its relevance for surgery planning, especially when considering lymphadenectomy and the associated differences in terms of risk of recurrence and prognosis [6]. Imaging derived biomarkers are often used in clinical and research settings, as objective, non-invasive indicators of biological, pathological and prognostic factors. The most widely used in EC are the SUV for PET imaging and ADC for MRI. In particular, SUVmax is correlated with tumor aggressiveness and prognosis, while ADCmin is useful for outcome prediction [28–31].

In our patient population, hybrid 18F-FDG PET/MRI correctly detected all primary tumors and had a good accuracy in detecting myometrial invasion (77%) and a high accuracy in detecting lymph node involvement (91%). Volume MRI imaging derived parameters (Volume index, TTV, TVR) and PET-derived

MTV40 and TLG40 can predict LVSI and MRI volume parameters can correctly stratify patients with high- versus low- risk profiles before surgery.

These quantitative evaluations could play a decisive role in planning therapeutic and surgical choice in view of personalized treatment approaches.

Previous studies have demonstrated a relevant role of the combined use of both 18F-FDG PET and MRI in the staging setting of endometrial cancer. For instance, our group demonstrated a synergic ability of these two imaging modalities, used separately, in providing an accurate staging of EC, also identifying correlations between PET and MRI derived parameters [32–34].

However, very few studies have investigated the accuracy and predictive value of simultaneous 18F-FDG PET/MRI in the staging setting of endometrial cancer, so far. Volume index, TLG and SUVmax/ADCmean ratio derived from distinct MRI and PET scans predict myometrial invasion and lymph node involvement or disease recurrence [21, 27, 32–34].

Only two studies [35, 36] investigated the diagnostic accuracy of fully-integrated 18F-FDG PET/MRI in population of patients affected by only endometrial cancer; the remaining studies included the assessment of heterogenous gynaecological malignancies. Tsuyoshi et al. [35], reported a diagnostic accuracy of 91.3% of 18F-FDG PET/MRI in staging lymph node involvement in a population of 36 patients with endometrial cancer. Bian et al. [36] retrospectively reported a sensitivity of 100% for 18F-FDG PET/MRI in detecting the primary tumor and an accuracy of 81.8% in delineating myometrial invasion; the slightly higher percentage of detection compared to our results may be related to the retrospective design of the study [36].

The predictive role of tumor size in patients with endometrial cancer has been also previously demonstrated. The FIGO staging system considers tumor size as one of the standard measurements for cervical cancer, but not for endometrial cancer [8] even though its prognostic value can be traced back to the second half of the last century, when Gusberg et al. [37] demonstrated positive correlation between tumor size and poor prognosis. Schink et al. [38] used average tumor diameter to predict lymph node involvement and survival; tumors > 2 cm were correlated to higher rate of lymph node metastasis (15% vs 4% ≤ 2 cm) and lower survival (98% 5-year survival for patients with tumors ≤ 2; 84% 5-year survival > 2 cm). Mariani et al. [39] reported that there was a significant difference in prognosis for patients with low-risk endometrial cancer and tumor size (< 2 cm and ≥ 2 cm). Myometrial invasion, histology and tumor size are also used in the Mayo criteria for risk assessment [40].

Our data shows that volume index (> 15.29) is associated with high-risk tumor and a volume index > 25.45 is also predictive for LVSI. This is coherent with what reported in literature where high volume index is associated to occurrence of lymph node metastases [41] and poor prognosis [42]. The ratio between tumor and uterine volume (TVR) > 21.1 was associated with lymphovascular space invasion; a value very similar to that found by Nougaret et al. [43] in which the cut-off was ≥ 25.36.

In our sample, no association was observed between MRI diffusion parameters and histology (grade, LVSI, deep myometrial invasion, risk or p53 expression), although this result could be due to the limited sample size. Similarly, Rechichi et al. [44] described that ADC had no correlation to grade and myometrial invasion. Shih et al. [34] described that ADCmin extrapolated from a fully integrated PET/MRI scan was associated to grade, stage and cervical invasion, but also these authors did not find a correlation with myometrial invasion and LVSI. Bharwani et al. [45] showed a non-statistically significant difference between tumor grades and ADCmin- and mean. ADC values were correlated to tumor grade by Tamai et al. [46] however, the authors described a certain overlap of ADC ranges for the different grades. Therefore, the correlation between ADC and tumor grade is still a matter of discussion.

Regarding risk groups, Tsuyoshi et al. [35] reported that high-risk cancers had a significantly lower ADC than low-risk cancers. These results are in contrast with those of our study, in which no association was found between these parameters. Further studies with larger patient numbers are needed to clarify the discording role of ADC in endometrial cancer.

Even though the most widely imaging biomarker in PET is SUVmax, usually associated with tumor aggressiveness and prognosis [28, 33, 34], this finding is not confirmed by our data with the actual sample size. However, we found a predictive value of MTV40 and TLG40 in assessing LVSI. An interesting and additive value of our study relies on the fact that we provided specific threshold of these metabolic parameters, able to indicate the presence of a higher risk of aggressiveness, as it is LVSI. No PET derived parameters were able to differentiate low- versus high-risk patients.

The limitation of the data presented may be the low number of our patients' cohort, yet this is only a preliminary analysis of a larger prospective population of endometrial cancer patients in which PET/MR images are simultaneously acquired. In addition, the low number of patients with lymph node involvement did not allow to well perform a statistical evaluation of the ability of hybrid imaging derived parameters in predicting this event.

In conclusion, fully integrated PET/MRI shows good to high accuracy in detecting myometrial invasion and lymph node involvement. Moreover, distinct quantitative parameters from this hybrid modality of imaging can predict the presence of LVSI and can correctly stratify patients according to the internationally accepted risk profiles.

Declarations

Compliance with ethical standards

Conflict of interest

The authors declare no conflict of interest.

Ethical approval

All procedures performed in studies involving human participants were in accordance with the ethical standards of the Institutional and national research committee and with the 1964 Helsinki Declaration and its later amendments or comparable ethical standards. In particular, patients' recruitment started after the approval by the Institutional Ethic Committee of San Raffaele Scientific Institute (protocol number 85/INT/2019).

Acknowledgments

Signa PET/MRI system (GEMS, Wakesha, Wisconsin, USA) used in the present work has been purchased with funding from Italian Ministry of Health.

The authors thank Stephanie Steidler for her contribution in critically reviewing the study proposal and participation in writing and technical editing of the manuscript.

The authors thank Tenace Nazario Pio for his assistance in selecting the histopathological images included in this manuscript.

References

1. Siegel RL, Miller KD, Jemal A. Cancer statistics, 2018. CA Cancer J Clin. 2018;

2. ACOG Practice Bulletin #65: Management of Endometrial Cancer. Obstet Gynecol. 2005;

3. Brüggmann D, Ouassou K, Klingelhöfer D, Bohlmann MK, Jaque J, Groneberg DA. Endometrial cancer: Mapping the global landscape of research. J Transl Med. 2020;

4. Salvesen HB, Haldorsen IS, Trovik J. Markers for individualised therapy in endometrial carcinoma. Lancet Oncol. 2012.

5. GLOBOCAN. The Global Cancer Observatory - All cancers. Int Agent Res Cancer - WHO. 2020;

6. Colombo N, Creutzberg C, Amant F, Bosse T, González-Martón A, Ledermann J, et al. ESMO-ESGO-ESTRO consensus conference on endometrial cancer: Diagnosis, treatment and follow-up. Ann Oncol. 2016;

7. Brooks RA, Fleming GF, Lastra RR, Lee NK, Moroney JW, Son CH, et al. Current recommendations and recent progress in endometrial cancer. CA Cancer J Clin, 2019;

8. CREASMAN W, ODICINO F, MAISONNEUVE P, QUINN M, BELLER U, BENEDET J, et al. Carcinoma of the Corpus Uteri. Int J Gynecol Obstet. 2006;

9. Greven KM, Randall M, Fanning J, Bahktar M, Duray P, Peters A, et al. Patterns of failure in patients with stage I, grade 3 carcinoma of the endometrium. Int J Radiat Oncol Biol Phys. 1990;

10. Straughn JM, Huh WK, Orr JW, Kelly FJ, Roland PY, Gold MA, et al. Stage IC adenocarcinoma of the endometrium: Survival comparisons of surgically staged patients with and without adjuvant radiation therapy. Gynecol Oncol. 2003;

11. Creutzberg CL, Van Putten WLJ, Wárláin-Rodenhtiis CC, Van Den Bergh ACM, De Winter KAJ, Koper PCM, et al. Outcome of high-risk stage IC, grade 3, compared with stage I endometrial carcinoma patients: The postoperative radiation therapy in endometrial carcinoma trial. J Clin Oncol. 2004;

12. Sagae S, Susumu N, Viswanathan AN, Aoki D, Backes FJ, Provencher DM, et al. Gynecologic cancer intergroup (GCIG) consensus review for uterine serous carcinoma. Int J Gynecol Cancer. 2014;

13. Getz G, Gabriel SB, Cibulskis K, Lander E, Sivachenko A, Sougnez C, et al. Integrated genomic characterization of endometrial carcinoma. Nature. 2013;

14. Helpman L, Kupets R, Covens A, Saad RS, Khalifa MA, Ismiil N, et al. Assessment of endometrial sampling as a predictor of final surgical pathology in endometrial cancer. Br J Cancer. 2014;

15. Daix M, Aida Angeles M, Migliorelli F, Kakkos A, Martinez Gomez C, Delbecque K, et al. Concordance between preoperative ESMO-ESGO-ESTRO risk classification and final histology in early-stage endometrial cancer. J Gynecol Oncol. 2021;

16. Colombo N, Preti E, Landoni F, Carinelli S, Colombo A, Marini C, et al. Endometrial cancer: ESMO clinical practice guidelines for diagnosis, treatment and follow-up. Ann Oncol. 2013;

17. Nougaret S, Horta M, Sala E, Lakhman Y, Thomassin-Naggara I, Kido A, et al. Endometrial Cancer MRI staging: Updated Guidelines of the European Society of Urogenital Radiology. Eur Radiol. 2019;

18. Picchio M, Mangili G, Samanes Gajate AM, De Marzi P, Spinapolice EG, Mapelli P, et al. High-grade endometrial cancer: Value of [18F]FDG PET/CT in preoperative staging. Nucl Med Commun. 2010;

19. Bollineni VR, Ytre-Hauge S, Bollineni-Balabay O, Salvesen HB, Haldorsen IS. High diagnostic value of 18F-FDG PET/CT in endometrial cancer: Systematic review and meta-analysis of the literature. J. Nucl. Med. 2016;

20. Kitajima K, Murakami K, Yamasaki E, Kaji Y, Sugimura K. Accuracy of integrated FDG-PET/contrast-enhanced CT in detecting pelvic and paraaortic lymph node metastasis in patients with uterine cancer. Eur Radiol. 2009;

21. Mapelli P, Ironi G, Bergamini A, Mangili G, Paola R, Taccagni GL, et al. Synergic role of preoperative 18F-fluorodeoxyglucose PET and MRI parameters in predicting histopathological features of endometrial cancer. Nucl Med Commun. 2020;

22. Crivellaro C, Landoni C, Elisei F, Buda A, Bonacina M, Grassi T, et al. Combining positron emission tomography/computed tomography, radiomics, and sentinel lymph node mapping for nodal staging of

endometrial cancer patients. Int J Gynecol Cancer. 2020;

23. Boellaard R, Delgado-Bolton R, Oyen WJG, Giammarile F, Tatsch K, Eschner W, et al. FDG PET/CT: EANM procedure guidelines for tumour imaging: version 2.0. Eur. J. Nucl. Med. Mol. Imaging. 2015;

24. Meissnitzer M, Forstner R. MRI of endometrium cancer - How we do it. Cancer Imaging. 2016;

25. Santaballa A, Matías-Guiu X, Redondo A, Carballo N, Gil M, Gómez C, et al. SEOM clinical guidelines for endometrial cancer (2017). Clin Transl Oncol. 2018;

26. Epstein E, Blomqvist L. Imaging in endometrial cancer. Best Pract Res Clin Obstet Gynaecol. 2014;

27. Eriksson LSE, Lindqvist PG, Flöter Rådestad A, Dueholm M, Fischerova D, Franchi D, et al. Transvaginal ultrasound assessment of myometrial and cervical stromal invasion in women with endometrial cancer: Interobserver reproducibility among ultrasound experts and gynecologists. Ultrasound Obstet Gynecol. 2015;

28. Nakamura K, Hongo A, Kodama J, Hiramatsu Y. The measurement of SUVmax of the primary tumor is predictive of prognosis for patients with endometrial cancer. Gynecol Oncol. 2011;

29. Mapelli P, Bergamini A, Fallanca F, Rancoita PMV, Cioffi R, Incerti E, et al. Prognostic role of FDG PET-derived parameters in preoperative staging of endometrial cancer. Rev Esp Med Nucl Imagen Mol. 2019;

30. Nakamura K, Imafuku N, Nishida T, Niwa I, Joja I, Hongo A, et al. Measurement of the minimum apparent diffusion coefficient (ADCmin) of the primary tumor and CA125 are predictive of disease recurrence for patients with endometrial cancer. Gynecol Oncol. 2012;

31. Inoue C, Fujii S, Kaneda S, Fukunaga T, Kaminou T, Kigawa J, et al. Correlation of apparent diffusion coefficient value with prognostic parameters of endometrioid carcinoma. J Magn Reson Imaging. 2015;

32. Nakamura K, Kodama J, Okumura Y, Hongo A, Kanazawa S, Hiramatsu Y. The SUVmax of 18F-FDG PET correlates with histological grade in endometrial cancer. Int J Gynecol Cancer. 2010;

33. Kitajima K, Kita M, Suzuki K, Senda M, Nakamoto Y, Sugimura K. Prognostic significance of SUVmax (maximum standardized uptake value) measured by [18F]FDG PET/CT in endometrial cancer. Eur J Nucl Med Mol Imaging. 2012;

34. Shih IL, Yen RF, Chen CA, Chen B Bin, Wei SY, Chang WC, et al. Standardized uptake value and apparent diffusion coefficient of endometrial cancer evaluated with integrated whole-body PET/MR: Correlation with pathological prognostic factors. J Magn Reson Imaging. 2015;

35. Tsuyoshi H, Tsujikawa T, Yamada S, Chino Y, Shinagawa A, Kurokawa T, et al. FDG-PET/MRI with high-resolution DWI characterises the distinct phenotypes of endometrial cancer. Clin Radiol. 2020;

36. Bian LH, Wang M, Gong J, Liu HH, Wang N, Wen N, et al. Comparison of integrated PET/MRI with PET/CT in evaluation of endometrial cancer: A retrospective analysis of 81 cases. PeerJ. 2019;

37. Gusberg SB, Jones HC, Tovell HMM. Selection of treatment for corpus cancer. Obstet Gynecol Surv. 1961;

38. Schink JC, Miller DS, Lurain JR, Rademaker AW. Tumor size in endometrial cancer. Cancer. 1991;

39. Mariani A, Webb MJ, Keeney GL, Haddock MG, Calori G, Podratz KC. Low-risk corpus cancer: Is lymphadenectomy or radiotherapy necessary? Am J Obstet Gynecol. 2000;

40. Milam MR, Java J, Walker JL, Metzinger DS, Parker LP, Coleman RL. Nodal metastasis risk in endometrioid endometrial cancer. Obstet Gynecol. 2012;

41. Todo Y, Choi HJ, Kang S, Kim JW, Nam JH, Watari H, et al. Clinical significance of tumor volume in endometrial cancer: A Japan-Korea cooperative study. Gynecol Oncol. 2013;

42. Todo Y, Watari H, Okamoto K, Hareyama H, Minobe S, Kato H, et al. Tumor volume successively reflects the state of disease progression in endometrial cancer. Gynecol Oncol. 2013;

43. Nougaret S, Reinhold C, Alsharif SS, Addley H, Arceneau J, Molinari N, et al. Endometrial cancer: Combined MR volumetry and diffusion-weighted imaging for assessment of myometrial and lymphovascular invasion and tumor grade. Radiology. 2015;

44. Rechichi G, Galimberti S, Signorelli M, Franzesi CT, Perego P, Valsecchi MG, et al. Endometrial cancer: Correlation of apparent diffusion coefficient with tumor grade, depth of myometrial invasion, and presence of lymph node metastases. Am J Roentgenol. 2011;

45. Bharwani N, Miquel ME, Sahdev A, Narayanan P, Malietzis G, Reznek RH, et al. Diffusion-weighted imaging in the assessment of tumour grade in endometrial cancer. Br J Radiol. 2011;

46. Tamai K, Koyama T, Saga T, Umeoka S, Mikami Y, Fujii S, et al. Diffusion-weighted MR imaging of uterine endometrial cancer. J Magn Reson Imaging. 2007;

Tables

Table 1. Patients' characteristics (n=35)

Characteristics	Frequency (%)
Age (years, mean; SD)	66.57 (10.21)
FIGO Stage	
IA	8 (22.9%)
IB	12 (34.3%)
II	4 (11.4%)
IIIA	3 (8.6%)
IIIC1	5 (14.3%)
IIIC2	1 (2.9%)
IV	2 (5.7%)
Tumor grade	
1	3 (8.6%)
2	21 (60.0%)
3	11 (31.4%)
Tumor Type	
1	28 (80.0%)
2	7 (20.0%)
Histology	
Endometrioid	28 (80.0%)
Serous	3 (8.6%)
Mixed serous/Endometroid	1 (2.8%)
Other (TMMN/squamocellular)	3 (8.6%)
Risk group	

Low risk	13 (37.1%)
High risk	22 (62.9%)

Table 2. MRI and PET variables (n=35)

Variables	Median [IQR]
MRI	
Volume Index (cc)	23.925 [7.664-98.48]
TTV (cc)	9.47 [3.5-42.65]
TVR (%)	19.464 [7.237-33.001]
ADCmean (10^{-3} mm^2/s)	0.96 [0.85-1.03]
ADCmin (10^{-3} mm^2/s)	0.63 [0.515-0.745]
PET	
SUVmax	21.51 [17.2-23.945]
SUVmean40	13.31 [11.03-14.7]
MTV40	9.39 [4.505-30.595]
TLG40	139.913 [38.959-434.851]

Table 3. ROC curve analyses

3a. Prediction of endometrial cancer risk group (22 medium-high risk vs 13 low risk patients)

	AUC analysis			threshold analysis		
Variable	**AUC value**	**p-value**	**adjusted p-value**	**threshold**	**sensitivity**	**specificity**
Volume Index	0.836	0.0007	**0.0059**	15.39	0.9091	0.7692
TTV	0.801	0.0026	**0.0235**	7.85	0.8182	0.7692
TVR	0.808	0.0020	**0.0181**	8.22	0.8636	0.6923
ADCmean	0.610	0.2893	1.0000	≤0.99	0.6818	0.6154
ADCmin	0.701	0.0515	0.4638	≤0.64	0.6364	0.6923
SUVmax	0.755	0.0133	0.1198	21.67	0.6818	0.8462
SUVmean40	0.774	0.0077	0.0697	12.90	0.7727	0.7692
MTV40	0.759	0.0107	0.0959	5.61	0.8636	0.6923
TLG40	0.759	0.0107	0.0959	82.33	0.8182	0.6923

3b. Prediction of LVSI (13 patients with LVSI vs 22 without)

	AUC analysis			threshold analysis		
Variable	**AUC value**	**p-value**	**adjusted p-value**	**threshold**	**sensitivity**	**specificity**
Volume Index	0.857	0.0003	**0.0023**	>25.45	0.9231	0.8182
TTV	0.832	0.0008	**0.0068**	>14.35	0.7692	0.8636
TVR	0.832	0.0008	**0.0068**	>21.08	0.7692	0.7727
ADCmean	0.603	0.3215	1.0000	≤0.99	0.7692	0.5455
ADCmin	0.666	0.1084	0.9755	≤0.64	0.6923	0.5909
SUVmax	0.563	0.5502	1.0000	>22.76	0.5385	0.6818
SUVmean40	0.617	0.2599	1.0000	>13.24	0.7692	0.5909
MTV40	0.853	0.0003	**0.0027**	>8.12	1.0000	0.7273
TLG40	0.815	0.0015	**0.0139**	>131.40	0.8462	0.6818

Table 3c. Prediction of deep myometrial invasion (22 patients with deep myometrial invasion, i.e. myometrial invasion >50%, vs 13 without)

	AUC analysis			threshold analysis		
Variable	**AUC value**	**p-value**	**adjusted p-value**	**threshold**	**sensitivity**	**specificity**
Volume Index	0.703	0.0487	0.4379	>25.45	0.5909	0.7692
TTV	0.689	0.0673	0.6058	>8.19	0.6818	0.6154
TVR	0.720	0.0315	0.2834	>7.57	0.8636	0.5385
ADCmean	0.570	0.5051	1.0000	≤1.02	0.7273	0.6154
ADCmin	0.610	0.2896	1.0000	≤0.60	0.5000	0.6923
SUVmax	0.545	0.6695	1.0000	>20.28	0.6818	0.4615
SUVmean40	0.566	0.5276	1.0000	>13.48	0.5000	0.6923
MTV40	0.647	0.1586	1.0000	>7.50	0.6818	0.6154
TLG40	0.643	0.1690	1.0000	>85.21	0.6818	0.5385

Table 3d. Prediction of p53 expression (13 patients with expression vs 22 without expression of p53)

	AUC analysis			threshold analysis		
Variable	**AUC value**	**p-value**	**adjusted p-value**	**threshold**	**sensitivity**	**specificity**
Volume Index	0.668	0.1055	0.9497	>24.44	0.7692	0.6818
TTV	0.671	0.0982	0.8838	>9.00	0.7692	0.6364
TVR	0.654	0.1391	1.0000	>21.08	0.6154	0.6818
ADCmean	0.696	0.0578	0.5203	>0.97	0.6923	0.6364
ADCmin	0.747	0.0168	0.1512	>0.66	0.7692	0.7727
SUVmax	0.624	0.2321	1.0000	>22.49	0.6154	0.6818
SUVmean40	0.642	0.1720	1.0000	>13.74	0.6154	0.7273
MTV40	0.612	0.2865	1.0000	>8.12	0.6923	0.5455
TLG40	0.615	0.2713	1.0000	>78.63	0.8462	0.4545

Table 3e. Prediction of grading (11 grading=3 vs 24 grading=1or2)

	AUC analysis			threshold analysis		
Variable	**AUC value**	**p-value**	**adjusted p-value**	**threshold**	**sensitivity**	**specificity**
Volume Index	0.648	0.1740	1.0000	25.45	0.6364	0.6250
TTV	0.621	0.2675	1.0000	8.19	0.7273	0.5000
TVR	0.587	0.4299	1.0000	21.08	0.5455	0.6250
ADCmean	0.530	0.7896	1.0000	≤0.95	0.5455	0.5000
ADCmin	0.540	0.7222	1.0000	≤0.64	0.5455	0.5417
SUVmax	0.756	0.0173	0.1554	22.76	0.8182	0.7917
SUVmean40	0.769	0.0122	0.1101	13.74	0.8182	0.7917
MTV40	0.580	0.4722	1.0000	7.50	0.7273	0.5000
TLG40	0.617	0.2832	1.0000	157.17	0.6364	0.5833

Figures

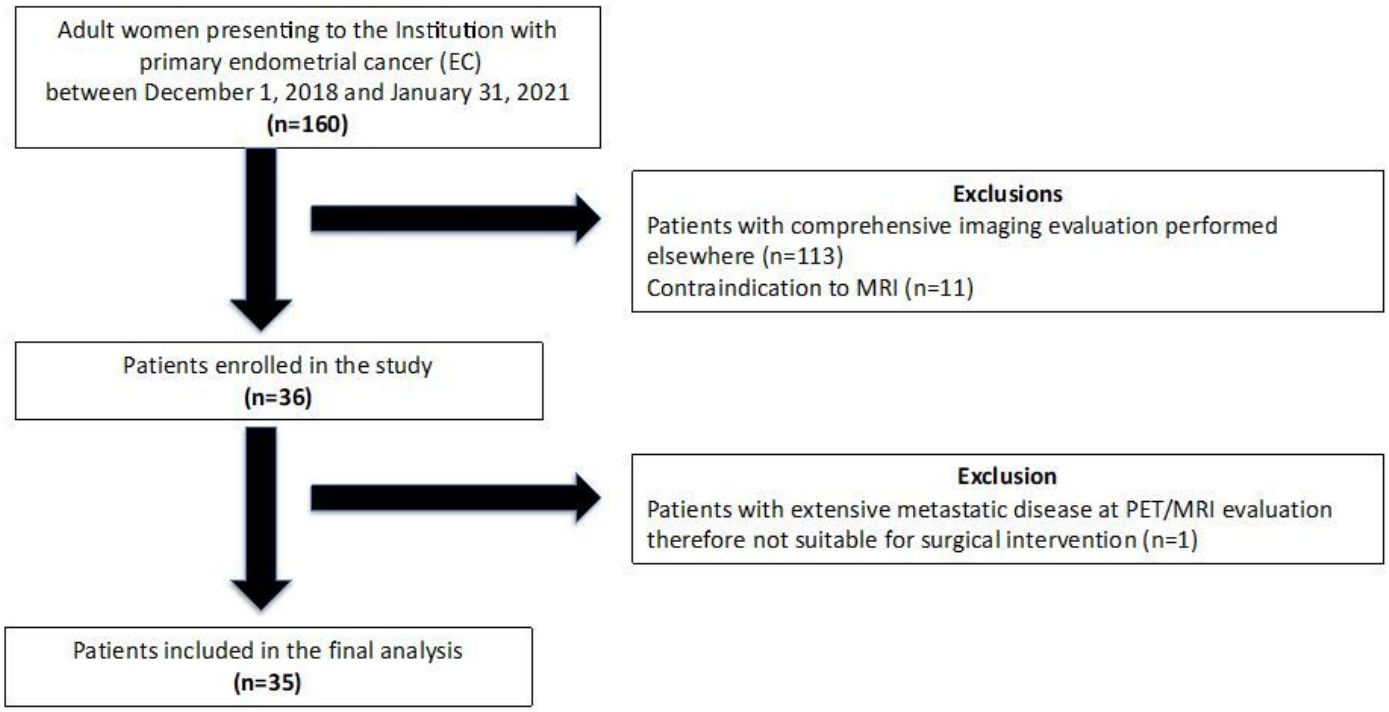

Figure 1

Flow diagram of our prospective single-Centre cohort study

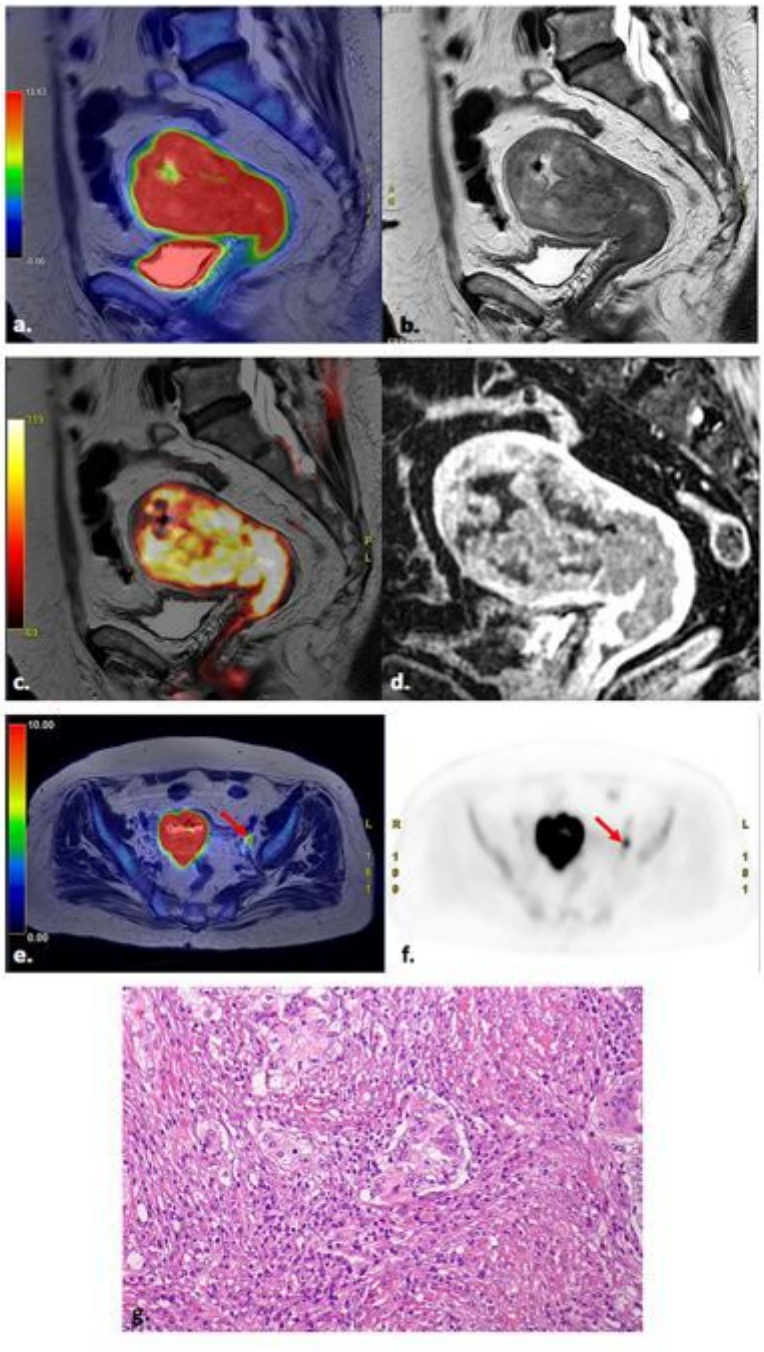

Figure 2

Image of a 78-year-old woman with endometrial cancer (stage IIIA, serous grade 3, LVSI positive, p53 positive, myometrial invasion > 50%). (a.) sagittal T2W-PET fused image, (b.) sagittal T2W image, (c.) sagittal T2W-DWI b1000 fused image, (d.) sagittal T1 post-contrast agent administration image, (e.) axial PET image fused with large field-of-view T2W image and (f.) axial PET image. Lymph-nodes metastases are indicated in e. and f. (arrows). Volume index: 249,69 cc; TTV: 100 cc; TVR: 81,3%; ADCmean: 0,89 x 10-3 mm2/s; ADCmin: 0,46 x 10-3 mm2/s. PET parameters of endometrial cancer: SUVmax: 25,09;

SUVmean: 13,97; MTV40: 71,07; TLG40: 992,84. (g.) Lympho-vascular neoplastic embolization constituted by large polygonal cells, with large nucleus with vescicular chromatin, sometimes voluminous nucleolus and with abundant clear cytoplasm (Haematoxylin and Eosin; 250x)

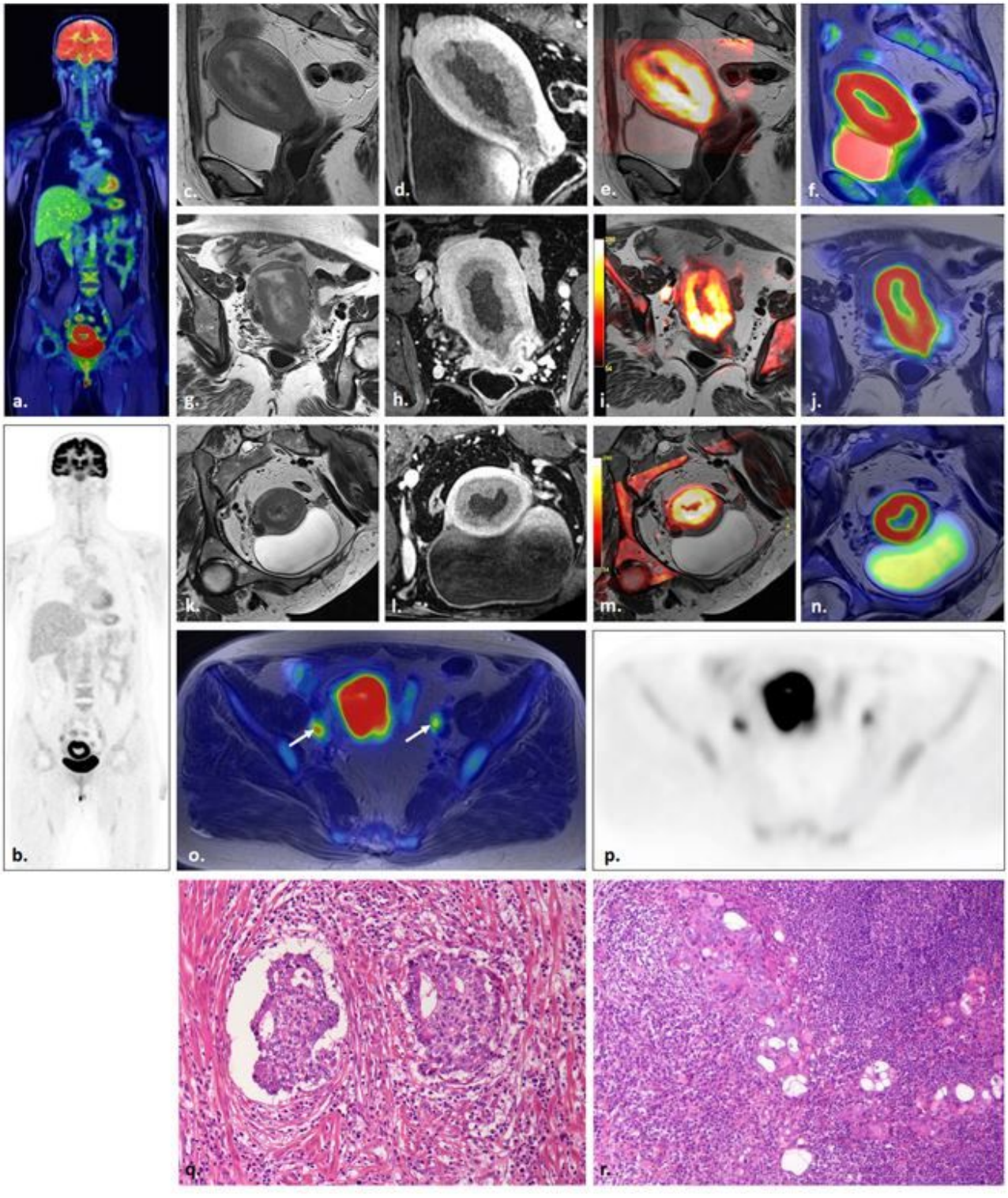

Figure 3

Image of a 54-year-old woman with endometrial cancer (stage IIIC1, endometrioid grade 2, LVSI positive, p53 positive, myometrial invasion > 50%). (a.) coronal whole body T1 fat suppression – PET fused

image, (b.) major intensity projection (MIP) of PET scan, (c.) sagittal T2 image , (d.) sagittal T1 post-contrast agent administration image, (e.) sagittal T2W-DWI b1000 fused image, (f.) sagittal T2W-PET fused image, (g.) coronal oblique T2, (h.) coronal oblique T1 post-contrast agent administration image, (i.) coronal oblique T2W-DWI b1000 fused image, (j.) coronal oblique T2W-PET fused image, (k.) axial oblique T2 image, (l.) axial oblique T1 post-contrast agent administration image, (m.) axial oblique T2W-DWI b1000 fused image, (n.) axial oblique T2W-PET fused image, (o.) axial large field-of-view T2W-PET fusion image, (p.) axial PET image. Volume index: 183 cc; TTV: 93 cc; TVR: 45%; ADCmean: 0,93 x 10-3 mm2/s; ADCmin: 0,55 x 10-3 mm2/s. PET parameters of endometrial cancer SUVmax 22,85; SUVmean: 14,4; MTV40: 71,26; TLG40: 1026,144. Lymph-nodes metastases are indicated in o. (arrows). (q.) Lympho-vascular neoplastic embolization (Haematoxylin-Eosin; 250 x). (r.) Lymph-nodal metastasis constituted by nests and cords of polygonal cells with a component of squamous metaplasia (Haematoxylin-Eosin;125x)